Why $\Xi(1690)$ and $\Xi(2120)$ are so narrow?

K. P. Khemchandani[1], A. Martínez Torres[2], A. Hosaka[3], H. Nagahiro[3,4], F. S. Navarra[2], and M. Nielsen[2]
[1] *Faculdade de Tecnologia, Universidade do Estado do Rio de Janeiro, Rod. Presidente Dutra Km 298, Pólo Industrial, 27537-000 , Resende, RJ, Brasil.*
[2] *Instituto de Física, Universidade de São Paulo, C.P 66318, 05314-970 São Paulo, SP, Brazil.*
[3] *Research Center for Nuclear Physics (RCNP), Mihogaoka 10-1, Ibaraki 567-0047, Japan.*
[4] *Department of Physics, Nara Women's University, Nara 630-8506, Japan.*
(Dated: August 26, 2016)

The Ξ baryons are expected to be naturally narrower as compared to their non-strange and strange counterparts since they have only one light quark and, thus, their decay involves producing either a light meson and doubly strange baryon or both meson and baryon with strangeness which involves, relatively, more energy. In fact, some Ξ's have full widths of the order of even 10-20 MeV when, in principle, they have a large phase space to decay to some open channels. Such is the case of $\Xi(1690)$, for which the width has been found to be of the order of 10 MeV in the latest BABAR and BELLE data. In this manuscript we study why some Ξ's are so narrow. Based on a coupled channel calculation of the pseudoscalar meson-baryon and vector meson-baryon systems with chiral and hidden local symmetry Lagrangians, we find that the answer lies in the intricate hadron dynamics. We find that the known mass, width, spin-parity and branching ratios of $\Xi(1690)$ can be naturally explained in terms of coupled channel meson-baryon dynamics. We find another narrow resonance which can be related to $\Xi(2120)$. We also look for exotic states Ξ^+ and Ξ^{--} but find none. In addition we provide the cross sections for $\bar{K}\Lambda, \bar{K}\Sigma \to \pi\Xi$ which can be useful for understanding the enhanced yield of Ξ reported in recent studies of heavy ion collisions.

arXiv:1608.07086v1 [nucl-th] 25 Aug 2016

I. INTRODUCTION

Little is known about Ξ resonances [1] since it is difficult to produce them in the laboratory directly. There are limited facilities around the world which have antikaon beams and a beam of nonstrange nature on a nucleon leads to low yields of Ξ baryons as two pairs of strange quarks are required to be produced in this case. However, efforts are being made to improve this situation. For example, the photoproduction of Ξ's on nucleons is being explored currently at the Jefferson laboratory [2] considering the possibility of the production of a hyperon resonance in the intermediate state, thus producing the strange quark pairs in two steps. Also, more information is expected to come in future from the J-PARC [3] and $\overline{\text{P}}$ANDA [4] facilities.

In addition, studies made by BELLE [5] and BABAR [6] collaborations show that it is possible to extract useful information on this subject from rare processes too. Specifically, some intriguing findings related to the properties of $\Xi(1690)$ have been reported in such studies. We find it useful to list these findings, and other relevant information on $\Xi(1690)$, in a separate subsection dedicated to $\Xi(1690)$ below.

A. $\Xi(1690)$

The first observation of $\Xi(1690)$ in the $\bar{K}\Sigma$ invariant mass spectrum was reported in Ref. [7], where the mass and width were determined to be $M = (1694 \pm 6)$ MeV, $\Gamma = (26 \pm 6)$ MeV in the negatively charged channel and $M = (1684 \pm 5)$ MeV, $\Gamma = (20 \pm 4)$ MeV in the neutral channel. The spin-parity of this state was not determined in Ref. [7]. Although the mass values obtained by the latest investigations [5, 6] are not very different, the width of $\Xi(1690)$ has been determined to be even narrower, of the order of 10 MeV [5, 6]. To mention explicit results, the BABAR collaboration deduced the mass and width of $\Xi(1690)$ to be: $M = \left(1684.7 \pm 1.3^{+2.2}_{-1.6}\right)$ MeV, $\Gamma = \left(8.1^{+3.9+1.0}_{-3.5-0.9}\right)$ MeV [6], and the BELLE Collaboration reported: $M = (1688 \pm 2)$ MeV, $\Gamma = (11 \pm 4)$ MeV [5]. Both studies obtained spin-parity of this state as $1/2^-$. It was also found in Ref. [6] that a clear evidence for $\Xi^0(1690)$ is found in the $\bar{K}^0\Lambda$ invariant mass spectrum but not in the $\pi^+\Xi^-$ spectrum. The information on the branching ratio of $\Xi^0(1690)$ to $\bar{K}\Lambda$ and $\bar{K}\Sigma$ has been updated in Ref. [5] to,

$$\frac{B(\Xi^0(1690) \to K^-\Sigma^+)}{B(\Xi^0(1690) \to \bar{K}^0\Lambda)} = 0.50 \pm 0.26. \qquad (1)$$

as compared to the value (1.8 ± 0.6) obtained from the older analysis of Ref. [7].

These properties are difficult to understand, for example, the narrow width of $\Xi(1690)$ in spite of having a large phase space to decay to open channels, like, $\pi\Xi$ and $\bar{K}\Lambda$. Similar is the case of the finding related to the suppressed decay to $\pi\Xi$, as compared to the decay to the $\bar{K}\Lambda$ channel (as is evident from the difficulty in the identification of the signal of $\Xi^0(1690)$ in the $\pi^+\Xi^-$ spectrum of Refs. [5, 6]). A light quark pair production, within a naïve quark model, is equivalently required in both cases (as can be seen in Fig. 1). The branching fraction to the $\bar{K}\Sigma$ and $\bar{K}\Lambda$ channels (shown in Eq. (1)) is also counterintuitive: there is little phase space for decay to the former one and one would anticipate this ratio to be much smaller.

In fact, these experimental findings have motivated

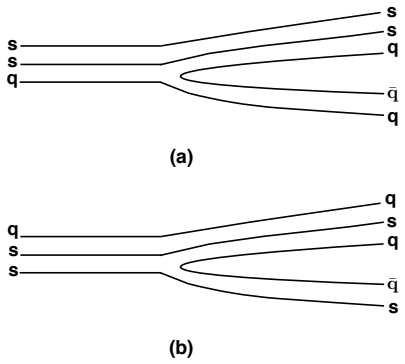

FIG. 1: Decay of a Ξ resonance to a meson ($q\bar{q}/s\bar{q}$)-baryon (qss/qqs) channel.

theoretical investigations within quark models, and the mass has been obtained: $M \sim 1725$ MeV [8]. Also, the decay properties of $\Xi(1690)$ have been studied within a chiral quark model [9], which includes hadron dynamics through a quark-meson effective coupling, and its total width was found to be 25 MeV. This value, although not widely different, is larger than the one observed in Refs. [5, 6]. Recently, the findings of the BES and the BELLE Collaborations motivated a study of $\Xi(1690)$ in terms of hadron degrees of freedom also [10]. The formalism used in Ref. [10], based on a t-channel interaction of pseudoscalar meson-baryon channels, reproduces well the mass of $\Xi(1690)$ but the width is found to be around 1 MeV. The author of Ref. [10] suggested that inclusion of more diagrams might be useful in obtaining a width of the order of 10 MeV.

In view of the growing interest in the Ξ-baryons at the experimental facilities, we find it timely to study cascade resonances in meson-baryon coupled systems. Our formalism includes interaction of both pseudoscalar as well vector mesons, and in the latter case we include s-, t-, u-channel diagrams and a contact term, whose origin will be explained in a subsequent section. As we shall show in this article, in agreement with Ref. [10], $\Xi(1690)$ can be understood as a state generated due to meson-baryon coupled channel dynamics and it is possible to straightforwardly understand all the experimental results reported in Refs. [5, 6]. A hadronic dynamical origin of resonances was predicted long time ago by Törnqvist [11] and the possibility of understanding some Ξ baryons (including $\Xi(1690)$) in terms of hadron dynamics has been discussed earlier in the literature [12–20]. We will compare our results with those obtained in such previous studies in this manuscript.

As we shall discuss, we find an evidence for another Ξ resonance, which is also narrower than expected (due to the existence of several open channels for decay) and can be related to $\Xi(2120)$. We find that the nature of this state is such that it can be difficult to identify its presence in the experimental data. We suggest possible ways to detect $\Xi(2120)$.

B. $\Xi(2120)$

Before proceeding further, for the sake of completeness, we find it useful to present the known information on $\Xi(2120)$ as well. Not much information is available on this resonance. Its spin-parity is not known. This state was first found in $\bar{K}\Lambda$ mass spectrum in Ref. [21], which reported its mass and width values to be $M = 2123 \pm 7$ MeV and $\Gamma = 25 \pm 12$ MeV. One of the later investigation confirmed an accumulation of events around 2120 MeV in $\bar{K}\Lambda$ and determined the mass and width to be $M = 2137 \pm 4$ MeV and $\Gamma \sim 20$ MeV [22]. This state was, however, not found in Ref. [23]. All these experimental data suffer from poor statistics. A better quality data is required to determine the properties of Ξ's with mass above 2 GeV. Indications of the existence of Ξ resonances around 2120 MeV, whose origin lies in the meson-baryon coupled channel dynamics, has been discussed in some previous works. For example, in Ref. [16], a pole around 2100 MeV is found with a full width of ~ 100 MeV for a Ξ, with $J^\pi = 1/2^-$ and $3/2^-$, as a result of pseudoscalar and vector meson-baryon interaction treated within a $SU(6)$ symmetry. In Ref. [15] also a Ξ with $J^\pi = 1/2^-$ and $3/2^-$, with mass ~ 2100 MeV and width ~ 60 MeV is found to get generated from meson-baryon dynamics. As we will show, we find the width of $\Xi(2120)$ to be narrower.

We discuss the details of our formalism and results in the next sections. In the discussions on the results, we will show that the presence of resonances affects the cross sections of processes like $\bar{K}\Lambda \to \pi\Xi$ and $\bar{K}\Sigma \to \pi\Xi$, which can be important in understanding the enhanced Ξ production found in the Ar + KCl collisions by the HADES collaboration [24].

II. FORMALISM

The formalism of the present study is based on solving the Bethe-Salpeter equation in a coupled channel approach. To do this we consider all systems with strangeness -2 formed by a pseudoscalar/vector meson with an octet baryon: $\pi\Xi$, $\eta\Xi$, $\bar{K}\Sigma$, $\bar{K}\Lambda$, $\rho\Xi$, $\omega\Xi$, $\phi\Xi$, $\bar{K}^*\Sigma$ and $\bar{K}^*\Lambda$.

We obtain the amplitudes for different transitions among these channels using Lagrangians based on effective field theories. To determine the vector-meson–baryon interaction we use the formalism developed in our previous work [28]. A detailed analysis of the low energy vector meson interaction with octet baryons was carried out in Ref [28] by calculating s-, t- and u-channel diagrams and a contact interaction, using a Lagrangian invariant under the gauge transformations of the hidden-local symmetry. It was found that the contribution of all the diagrams is of comparable size and that the full (summed) amplitude depended on the total spin as well as the isospin of the system. Following Ref. [28], thus, we write vector-baryon (VB) amplitudes for each spin-

isospin configuration as

$$V_{\rm VB}^{I,S} = V_{t,\rm VB}^{I,S} + V_{s,\rm VB}^{I,S} + V_{u,\rm VB}^{I,S} + V_{\rm CT,VB}^{I,S}. \quad (2)$$

These amplitudes can be obtained from the general Lagrangian

$$\mathcal{L}_{\rm VB} = -g\Bigg\{ \langle \bar{B}\gamma_\mu \left[V_8^\mu, B\right]\rangle + \langle \bar{B}\gamma_\mu B\rangle\langle V_8^\mu\rangle \quad (3)$$
$$+\frac{1}{4M}\left(F\langle \bar{B}\sigma_{\mu\nu}\left[V_8^{\mu\nu}, B\right]\rangle + D\langle \bar{B}\sigma_{\mu\nu}\left\{V_8^{\mu\nu}, B\right\}\rangle\right)$$
$$+\langle \bar{B}\gamma_\mu B\rangle\langle V_0^\mu\rangle + \frac{C_0}{4M}\langle \bar{B}\sigma_{\mu\nu}V_0^{\mu\nu}B\rangle\Bigg\},$$

where $\langle ...\rangle$ refers to an $SU(3)$ trace, the subscript 8 (0) on the meson fields denotes the octet (singlet) part of their wave function (relevant in case of ω and ϕ, for which we assume an ideal mixing). $V^{\mu\nu}$ represents the tensor field of the vector mesons,

$$V^{\mu\nu} = \partial^\mu V^\nu - \partial^\nu V^\mu + ig\left[V^\mu, V^\nu\right], \quad (4)$$

where V and B denote the SU(3) matrices for the (physical) vector mesons and octet baryons

$$V = \frac{1}{2}\begin{pmatrix} \rho^0+\omega & \sqrt{2}\rho^+ & \sqrt{2}K^{*^+} \\ \sqrt{2}\rho^- & -\rho^0+\omega & \sqrt{2}K^{*^0} \\ \sqrt{2}K^{*^-} & \sqrt{2}\bar{K}^{*^0} & \sqrt{2}\phi \end{pmatrix}; \quad (5)$$

$$B = \begin{pmatrix} \frac{1}{\sqrt{6}}\Lambda + \frac{1}{\sqrt{2}}\Sigma^0 & \Sigma^+ & p \\ \Sigma^- & \frac{1}{\sqrt{6}}\Lambda - \frac{1}{\sqrt{2}}\Sigma^0 & n \\ \Xi^- & \Xi^0 & -\sqrt{\frac{2}{3}}\Lambda \end{pmatrix}. \quad (6)$$

In Eq.(3), the coupling g is related to meson decay constants as

$$g = \frac{m}{\sqrt{2}f}, \quad (7)$$

and the constants $D = 2.4$, $F = 0.82$ and $C_0 = 3F - D$ are such that the anomalous magnetic couplings of ρNN, ωNN and ϕNN vertices are correctly reproduced. These values have also been found useful in calculations of the magnetic moments of the baryons in Ref. [29].

It is easy to see that a contact interaction arises from the commutator part of the tensor field (Eq. (4)). The resulting amplitude has a form

$$V_{\rm CT,VB}^{I,S} = i\, C_{\rm CT,VB}^I \frac{g_1 g_2}{2\sqrt{M_1 M_2}}\, \vec{\sigma}\cdot\vec{\epsilon_2}\times\vec{\epsilon_1}, \quad (8)$$

where M_1 (M_2) is the mass of the baryon in the initial (final) state, ϵ_1 (ϵ_2) represents the polarization vector of the vector meson in the initial (final) state, and $C_{\rm CT,VB}^I$ are isospin dependent coefficients whose values are given in the Appendix, in Tables IV, V for the different relevant channels. In Eq. (8) g_1 (g_2) is related to the decay constant of the vector meson in the initial (final) state through Eq. (7). We recall that the main purpose of the present article is to study the formation of resonances in a coupled meson-baryon system. We are, thus, interested in low energy dynamics of such a system and, as is customary, obtain all the amplitudes within a nonrelativistic approach.

Using the Yukawa-type vertices obtained from Eq. (3), the s- and u-channel amplitudes are deduced to be

$$V_{s,\rm VB}^{I,S} = C_{s,\rm VB}^I \left(\frac{g_1 g_2}{2\bar{M}+\bar{m}}\right)\vec{\epsilon}_2\cdot\vec{\sigma}\ \vec{\epsilon}_1\cdot\vec{\sigma}, \quad (9)$$

$$V_{u,\rm VB}^{I,S} = C_{u,\rm VB}^I \left(\frac{g_1 g_2}{2\bar{M}-\bar{m}}\right)\vec{\epsilon}_1\cdot\vec{\sigma}\ \vec{\epsilon}_2\cdot\vec{\sigma}, \quad (10)$$

where SU(3) averaged masses of baryons and vector mesons, respectively, are used for $\bar{M}$ and $\bar{m}$, for practical purposes. To obtain these amplitudes we consider the exchange of octet baryons. Thus, s-channel diagram (Eq. (9)) is null for the configurations with isospin 3/2 or spin 3/2. The values of the isospin coefficients $C_{s,\rm VB}^{1/2}$ and $C_{u,\rm VB}^I$ are given in the Appendix, in Table VI, and Tables VII, VIII, respectively.

The amplitudes for the t-channel are obtained, as in Ref. [15],

$$V_{t,\rm VB}^{I,S} = -\frac{C_{t,VB}^I}{4f_V^2}(\omega+\omega')\vec{\epsilon}_1\cdot\vec{\epsilon}_2, \quad (11)$$

where $\omega(\omega')$ and $\epsilon_1(\epsilon_2)$ are the energy and the polarization vector of the meson in the initial (final) state, respectively. The values of $C_{t,VB}^I$ are as given in Ref. [15]. As can be seen, this amplitude contributes equally to spin 1/2 as well as spin 3/2 configurations. Thus, the consideration of t-channel alone would result in spin-degenerate amplitudes, as found in Refs. [13–17]. However, such a degeneracy is removed by summing Eqs. (8), (9), (10) to the t-channel amplitude, giving rise to a spin, isospin-dependent results. Although, sometimes, it is possible that the interaction of a vector meson with a baryon may depend weakly on spin configurations (as can be seen from Tables IV-VIII given in the appendix), we find that this is not always the case. For example, the contact-term (Eq. (8)) for the $\rho\Xi$ diagonal amplitude, or for the transition of $\bar{K}^*\Lambda$ to $\rho\Xi$, $\omega\Xi$, $\phi\Xi$ is small, but the same is comparable, or even larger than the t-channel amplitude for $\bar{K}^*\Sigma \to \bar{K}^*\Sigma, \bar{K}^*\Lambda, \rho\Xi, \omega\Xi, \phi\Xi$. For a numerical comparison, we show the lowest order amplitudes obtained in the present work for the $\rho\Xi$ and $\bar{K}^*\Sigma$ channels in Fig. 2. In fact, the general spin-dependence of the vector meson-baryon kernels may be expected since both the interacting hadrons have nonzero spin and similar masses. An alternative mechanism of breaking the spin-degeneracy has been suggested in Ref. [19]. Further, we go a step forward by including pseudoscalar-baryon as coupled channels in our formalism. The consideration of various contributions to the vector-baryon amplitudes, together with the

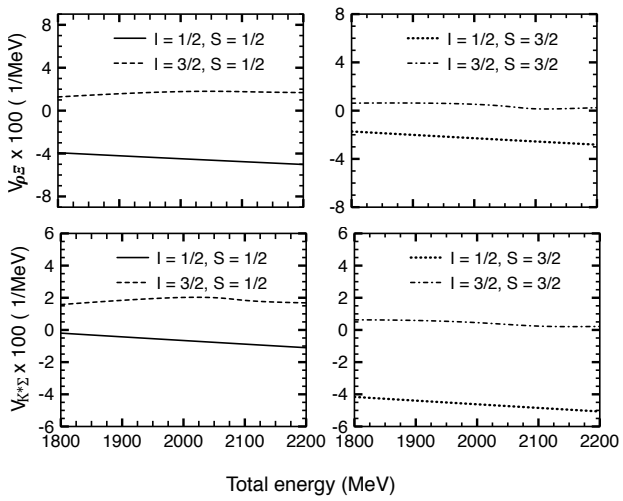

FIG. 2: A comparison of the lowest order $\rho\Xi$ and $\bar{K}^*\Sigma$ amplitudes (Eq. (2)) for different spin-isospin configurations.

treatment of the vector- and pseudoscalar-mesons at par in the coupled channel dynamics, is the distinct feature of our formalism.

Next, we discuss the amplitudes for transition between the pseudoscalar-baryon and vector-baryon channels. A formalism to obtain such amplitudes was developed in our previous work [30], where the Kroll-Ruderman term for the photoproduction of a pion was modified, in consistency with the the vector meson dominance phenomenon, by replacing the photon by a vector meson. The deduction was extended to the SU(3) case in Ref. [30] to obtain a general Lagrangian for the transitions among pseudoscalar-baryon (PB) and VB (vector-baryon) channels

$$\mathcal{L}_{\rm PBVB} = \frac{-ig_{KR}}{2f_\pi}\left(F'\langle\bar{B}\gamma_\mu\gamma_5\left[[P,V^\mu],B\right]\rangle + D'\langle\bar{B}\gamma_\mu\gamma_5\left\{[P,V^\mu],B\right\}\rangle\right), \quad (12)$$

where $F' = 0.46$, $D' = 0.8$, reproduce the axial coupling constant of the nucleon: $F' + D' \simeq g_A = 1.26$ [30].

In the present work we need the transition amplitudes between pseudoscalar-baryon and vector-baryon channels with strangeness -2. We obtain them using Eq. (12) to get

$$V^I_{\rm PBVB} = -i\,C^I_{\rm PBVB}\frac{g_{\rm KR}}{2\sqrt{f_P f_V}}\vec{\sigma}\cdot\vec{\epsilon}, \quad (13)$$

where $g_{\rm KR}$ is defined as the Kroll-Ruderman coupling [30]

$$g_{\rm KR} = \frac{m_V}{\sqrt{2f_P f_V}}, \quad (14)$$

and where m_V, f_P and f_V denote the mass of the vector meson, the decay constants of the pseudoscalar- and vector-meson, respectively, in each channel. The values of the decay constants used in our work are: $f_\pi = 93$ MeV, $f_\eta = 120.9$ MeV, $f_k = 113.46$ MeV, f_ρ, $f_\omega = 153.45$, $f_\phi = 168.33$ MeV, $f_{K^*} = 159.96$ MeV [31, 32]. The values of the isospin coefficients $C^I_{\rm PBVB}$ for isospin 1/2 and 3/2 are listed in Table X and IX in the appendix, respectively. The PB $\leftrightarrow$ VB transitions given by Eq. (13) for both isospin configurations are spin 1/2 amplitudes. The PB $\leftrightarrow$ VB transitions for total spin 3/2 is zero (as in Refs. [30, 33, 34]). This is consistent with the results obtained within a different formalism [19], where the VB amplitudes in spin 3/2 have been found to change weakly when coupled to pseudoscalar baryon systems.

Finally, the pseudoscalar meson-baryon amplitudes are obtained from the lowest order chiral Lagrangian [35, 36]

$$\mathcal{L}_{PB} = \langle\bar{B}i\gamma^\mu\partial_\mu B + \bar{B}i\gamma^\mu[\Gamma_\mu,B]\rangle - M_B\langle\bar{B}B\rangle + \frac{1}{2}D'\langle\bar{B}\gamma^\mu\gamma_5\{u_\mu,B\}\rangle + \frac{1}{2}F'\langle\bar{B}\gamma^\mu\gamma_5[u_\mu,B]\rangle, \quad (15)$$

where

$$\Gamma_\mu = \frac{1}{2}\left(u^\dagger\partial_\mu u + u\partial_\mu u^\dagger\right),\ u_\mu = iu^\dagger\partial_\mu U u^\dagger,$$
$$U = u^2 = exp\left(i\frac{P}{f_P}\right). \quad (16)$$

As defined earlier, f_P in Eq. (16) is the pseudoscalar decay constant, and P is

$$P = \begin{pmatrix} \pi^0 + \frac{1}{\sqrt{3}}\eta & \sqrt{2}\pi^+ & \sqrt{2}K^+ \\ \sqrt{2}\pi^- & -\pi^0 + \frac{1}{\sqrt{3}}\eta & \sqrt{2}K^0 \\ \sqrt{2}K^- & \sqrt{2}\bar{K}^0 & \frac{-2}{\sqrt{3}}\eta \end{pmatrix}$$

The resulting amplitudes are consistent with those obtained earlier in Ref. [12],

$$V^I_{PB} = -\frac{C^I_{PB}}{4f_1 f_2}\left(2\sqrt{s} - M_1 - M_2\right)\sqrt{\frac{(M_1+E_1)(M_2+E_2)}{4M_1M_2}}, \quad (17)$$

where M_1 (M_2), E_1 (E_2) represent the mass and energy of the baryon in the initial (final) state, respectively, and f_1 (f_2) is the decay constant of the meson in the initial (final) state. We do not give the values of C^I_{PB} here since they are same as those given in Ref. [12].

With the kernels prepared we solve the Bethe-Salpeter equation, in its on-shell factorization form [37, 38]

$$T = (1 - VG)^{-1}V, \quad (18)$$

where G is a loop of two hadrons which is divergent in nature. It is possible to evaluate the loop function by using the dimensional regularization or with a three-momentum cut-off. In the former case, the subtraction constants can be fixed to have natural values following Refs. [16, 39, 40], to ensure the interpretation of the resonances found in the calculations as those arising from the dynamics of the system. In the latter case, a cut-off

parameter Λ is used to regularize the loop function using a Gaussian form factor as

$$G = \int_0^\infty \frac{d^3q}{(2\pi)^3} \frac{1}{2E_1(\vec{q})} \frac{2M}{2E_2(\vec{q})} \frac{e^{\left[-\left(q^2-q_{on}^2\right)/\Lambda^2\right]}}{\sqrt{s}-E_1(\vec{q})-E_2(\vec{q})}, \tag{19}$$

where q_{on} is the three momentum of the relative motion of the particle in the intermediate state when they are on mass shell. We have calculated the amplitudes using both methods and find that the results obtained and conclusions are very similar. In the following we show the results obtained by calculating the loop function using Eq. (19) with $\Lambda = 800$ MeV, although, later on, we will present the values of the poles found within the dimensional regularization scheme too.

III. RESULTS AND DISCUSSIONS

A. Isospin = 1/2 and Spin =1/2

We begin the discussion of the results by showing the squared amplitudes for different coupled channels in the isospin 1/2, spin 1/2 configuration in Fig. 3. It can be

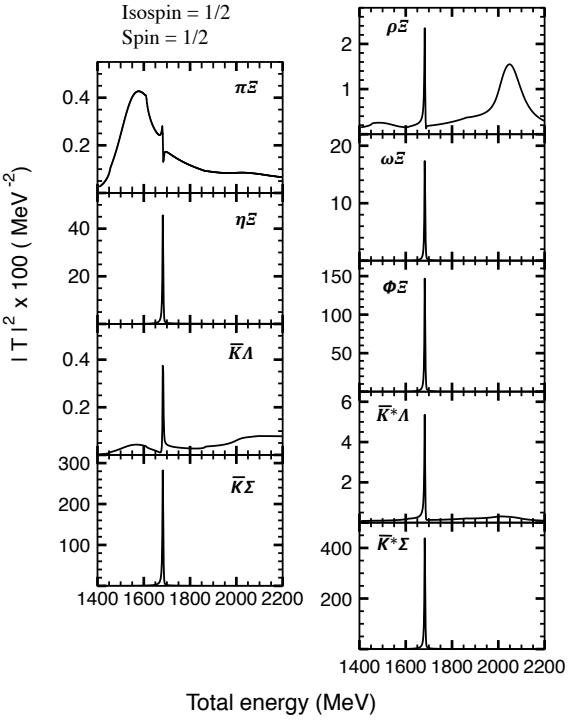

FIG. 3: Squared amplitudes for the total isospin and spin 1/2.

seen from Fig. 3 that a clear narrow peak is present around 1690 MeV in all the channels except in $\pi\Xi$. This peak corresponds to a pole in the complex plane at

$$M - i\Gamma/2 = 1682 - i3 \text{ MeV}. \tag{20}$$

This pole position is in excellent agreement with the recently determined mass and width of $\Xi(1690)$ by the BABAR Collaboration: $M = \left(1684.7 \pm 1.3^{+2.2}_{-1.6}\right)$ MeV, $\Gamma = \left(8.1^{+3.9+1.0}_{-3.5-0.9}\right)$ MeV [6] and those determined by the BELLE Collaboration: $M = (1688 \pm 2)$ MeV, $\Gamma = (11 \pm 4)$ MeV [5]. The spin-parity $1/2^-$ also coincides with the experimental data analysis of Ref. [6]. The width in Eq. (20) is larger than the value ~ 1 MeV obtained in Ref. [10]. This is because the coupling of the vector-baryon channels pushes the pole to slightly lower energies, hence, bringing it slightly closer to the $\bar{K}\Lambda$ channel. This latter fact allows for a bigger decay width since the coupling of the pole to the $\bar{K}\Lambda$ channel increases.

We have also calculated the decay rates of our state to different open channels and we find the partial widths (in percentage) to $\pi\Xi$, $\bar{K}\Lambda$ and $\bar{K}\Sigma$ as 17.6%, 27.1% and 55.3%, respectively. Using these values we can see that the branching fraction defined by Eq. (1) is 0.49, which is remarkably similar to the experimental value [5].

Further, we show the coupling of the different channels to the state we associate with $\Xi(1690)$ in Table. I. It can be seen from the values of these couplings that

TABLE I: Couplings of different channels to $\Xi(1690)$.

Channels	Couplings
$\pi\Xi$	$-0.1 - i0.1$
$\eta\Xi$	$1.2 + i0.1$
$\bar{K}\Sigma$	$1.8 + i0.1$
$\bar{K}\Lambda$	$-0.3 + i0.1$
$\rho\Xi$	$0.5 - i0.1$
$\omega\Xi$	$-0.9 - i0.0$
$\phi\Xi$	$1.6 + i0.1$
$\bar{K}^*\Sigma$	$-2.0 - i0.2$
$\bar{K}^*\Lambda$	$0.6 - i0.1$

the pole given by Eq. (20) couples very weakly to $\pi\Xi$, thus, explaining the difficulty of identifying the state in the data on $\pi\Xi$ mass spectrum [6]. The small coupling of the state to $\bar{K}\Lambda$ and the stronger one to $\bar{K}\Sigma$, in spite of the presence of a larger phase space for decay to the former (thresholds of $\bar{K}\Lambda \sim 1612$ MeV, $\bar{K}\Sigma \sim 1689$ MeV), explains why the branching ratio given in Eq. (1) is larger than expected. Thus, all the findings related to $\Xi(1690)$ can be well explained within the coupled channel dynamics of meson-baryon systems which indicate that this state should be interpreted as a dynamically generated state. It should be mentioned that suggestions on the hadronic dynamical origin of $\Xi(1690)$ have also been made in Refs. [10, 13, 16, 20].

We have also solved Bethe-Salpeter equations by calculating the loop function within the dimensional regularization scheme by using natural values of the subtraction

constants:

$$\begin{array}{lll} a_{\pi\Xi} = -1.05 & a_{\eta\Xi} = -2.30 & a_{\bar{K}\Sigma} = -1.90 \\ a_{\bar{K}\Lambda} = -1.65 & a_{\rho\Xi} = -2.63 & a_{\omega\Xi} = -2.64 \\ a_{\phi\Xi} = -2.93 & a_{\bar{K}^*\Sigma} = -2.60 & a_{\bar{K}^*\Lambda} = -2.50. \end{array} \quad (21)$$

These constants have been obtained by using the condition

$$G[\mu = 630 \text{ MeV}, \sqrt{s} = \sqrt{s}_{thr,min}] = 0, \quad (22)$$

for all the channels, where $\sqrt{s}_{thr,min}$ is the lowest threshold. Such a calculation leads to a pole at $1686 - i2$ MeV, which is similar to Eq. (20). All other results obtained in our work are comparable in a similar way when obtained by using a cut-off or dimensional regularization to calculate the loop integrals. We, thus, would show only the results obtained with a cut-off in the following discussions.

As can be seen from Fig. 3, another peak like structure is seen around 2050 MeV, in the squared amplitude of $\rho\Xi$ in spin 1/2, isospin 1/2 configuration. However, the complex plane analysis shows that this peak corresponds to a virtual state. A slight increase in the cut-off can make it a bound state. In any case, the squared amplitudes on the real axis (and, thus, the cross-sections, the couplings of the state to different channels) do not change much with the cut-off. Hence, a bump in the cross sections would be seen in experimental data. We, thus, find it useful to give the couplings of this peak structure in Table II. We have obtained the mass, width and couplings of this state using the squared amplitudes on the real axis. The mass and width of this state can be summarized as

$$M + i\Gamma/2 = 2050 - i63 \ \text{ MeV}. \quad (23)$$

TABLE II: Couplings of different channels to the virtual state of Eq. (23).

Channels	Couplings
$\pi\Xi$	$-0.2 - i0.0$
$\eta\Xi$	$0.3 + i0.0$
$\bar{K}\Sigma$	$-0.3 + i0.1$
$\bar{K}\Lambda$	$-0.1 + i0.3$
$\rho\Xi$	$2.8 + i0.0$
$\omega\Xi$	$0.2 - i0.1$
$\phi\Xi$	$-0.3 + i0.2$
$\bar{K}^*\Sigma$	$0.0 + i0.1$
$\bar{K}^*\Lambda$	$-1.4 + i0.4$

The question that arises is if we can relate this peak structure with any known state. Two poorly known states around 2 GeV are listed in Ref [1]: $\Xi(2030)$ and $\Xi(2120)$. The former one seems to have a spin $J \geq 5/2$ [1]. The existence of the latter one is based on a signal found in the $\bar{K}\Lambda$ mass spectrum [1]. Although a bump around 2100 MeV (corresponding to Eq. (23)) is visible in our $\bar{K}\Lambda$ squared matrix shown in Fig. 3, this signal cannot be identified with $\Xi(2100)$ since the width of the latter state is much smaller ($\sim$ 20-30 MeV). Thus, with the available information, we cannot relate the bump seen around 2050 MeV in our spin and isospin 1/2 amplitudes. But our findings indicate that a bump near 2050 MeV with full width around 120 MeV should be seen in the $\rho\Xi(\pi\pi\Xi)$ and $\bar{K}^*\Lambda(\bar{K}\pi\Lambda)$ spectra (see couplings for $\rho\Xi$ and $\bar{K}^*\Lambda$ in Table II).

Before proceeding further, it should be mentioned that yet another pole appears in the spin, isospin 1/2 configuration but deep in the complex plane, around 1530 MeV, with full width around 200 MeV. A broad structure around this energy region is seen in the $\pi\Xi$ t-matrix (in Fig. 3). However, identifying such broad states in experimental data should be difficult, especially because a narrow $3/2^+$ resonance, $\Xi(1530)$, exists in this energy region. As an example, we show the $\pi\Xi$ mass spectrum in Fig. 4, for the process studied by the BABAR Collaboration, $\Lambda_c^+ \to \Xi^-\pi^+K^+$, is näively obtained as

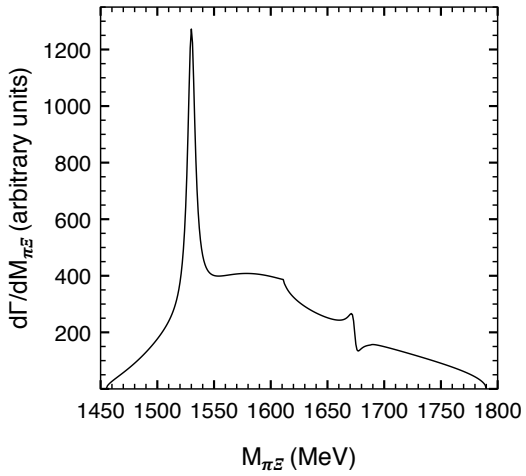

FIG. 4: The $\pi\Xi$ mass spectrum in the process $\Lambda_c^+ \to \Xi^-\pi^+K^+$ obtained by summing a Breit-Wigner distribution for the $\Xi(1530)$ resonance to the s-wave t-matrix obtained in the present work. It is possible to notice the presence of a structure around 1690 MeV and a $K\Lambda$ cusp around 1612 MeV.

$$\frac{d\Gamma}{dM_{\pi\Xi}} \propto p_K \; p_{\pi\Xi} \mid \mathcal{T}_{\pi\Xi} \mid^2 . \quad (24)$$

Here, p_K and $p_{\pi\Xi}$ represent the momentum of the kaon in the $\Xi^-\pi^+K^+$ system and the center of mass momentum in the $\pi\Xi$ subsystem, respectively. The matrix element, $\mathcal{T}_{\pi\Xi}$, in Eq. (24) is

$$\mid \mathcal{T}_{\pi\Xi} \mid^2 = \mid T_{\text{s}-wave} \mid^2 + \mid T_{\text{p}-wave} \mid^2 \quad (25)$$

We calculate Eq. (25) by using our amplitude for the s-wave part and by writing a Breit-Wigner function for the

p-wave ($\Xi(1530)$)

$$T_{\mathrm{p}-wave} = \frac{g^2}{\sqrt{s} - M_R + i\Gamma/2}. \quad (26)$$

We use $M_R = 1530$ MeV and $\Gamma/2 = 5$ MeV for $\Xi(1530)$, following Ref. [1], and estimate the coupling $g^2 \sim 0.47$ by assuming the decay rate $\Xi(1530) \to \pi\Xi$ to be nearly 100% [1].

B. Isospin = 1/2 and Spin =3/2

Next, we show the squared amplitudes for the isospin 1/2 and spin 3/2 configurations in Fig. 5. In this case

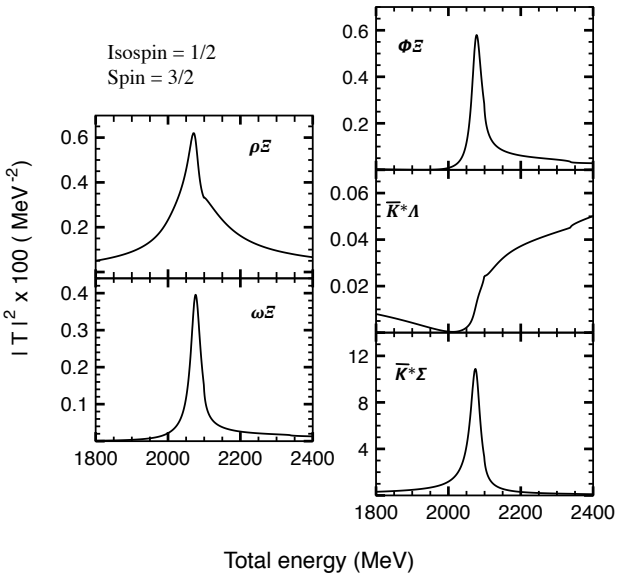

FIG. 5: Squared amplitudes for the total isospin 1/2 and spin 3/2.

a resonance is found at $M - i\Gamma/2 = 2078 - i17$ MeV, which couples strongly to the $\bar{K}^*\Sigma$ channel. Once again we come across a Ξ with a narrow width in spite of the availability of a large phase space to decay. In fact the decay width of this Ξ is mostly through the decay of K^*, and the corresponding pole goes to the real axis (and becomes a bound state) if the width of K^* is considered to be zero. The mass and width of this state are in good agreement with those of the known $\Xi(2120)$ state indicating its spin-parity to be $J^\pi = 3/2^-$. It should mainly decay to $\bar{K}^*\Sigma \to \bar{K}\pi\Sigma$, and through intermediate loops to $\bar{K}\Sigma$, $\pi\Xi$ channels (see Fig. 6). Such investigations should be made in detail in future. It is important to recall that a broader state with $J^\pi = 1/2^-$ is also found in our work, which, however, couples very weakly to the $\bar{K}^*\Sigma$ channel and should be found in $\rho\Xi$ or $\bar{K}^*\Lambda$ ($\rho\Xi \to \pi\pi\Xi$, $\rho\Xi \to \pi\Xi$, $\bar{K}^*\Lambda \to \bar{K}\pi\Lambda$) decay. In Table III, we provide the couplings of different channels to our spin 3/2 resonance, which we relate with $\Xi(2120)$.

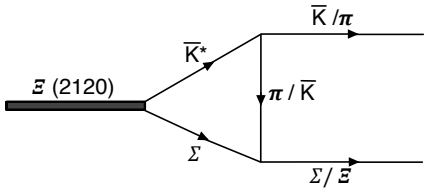

FIG. 6: Possible decay channels of $\Xi(2120)$.

TABLE III: Couplings of different channels to $\Xi(2120)$.

Channels	Couplings
$\rho\Xi$	$-0.73 + i0.0$
$\omega\Xi$	$1.1 + i0.0$
$\phi\Xi$	$-1.2 + i0.0$
$\bar{K}^*\Sigma$	$2.4 + i0.0$
$\bar{K}^*\Lambda$	$-0.3 + i0.1$

We also calculate isospin 3/2 amplitudes for spin 1/2 and 3/2 but find no resonance in such configurations, thus, implying absence of any exotic states in our study. A claim of the existence of a narrow, exotic Ξ^{--} state, with mass ~ 1862 MeV, in the $\pi^-\Xi^-$ mass spectrum was reported in Ref. [41]. However, later investigations have failed to confirm the existence of this state (see Ref. [42] for some recent results on this topic).

Finally, we have checked the stability of our results against the variation of the unique parameter of the calculation, which is the cut-off ($\Lambda = 800$ MeV) used to calculate the loop function (Eq. (19)). We change the value of Λ by ± 50 MeV and show, as an example, the variation of the squared amplitudes of the $\bar{K}\Sigma$ and $\bar{K}^*\Sigma$ channels in Figs 7 and 8, respectively. As can be seen

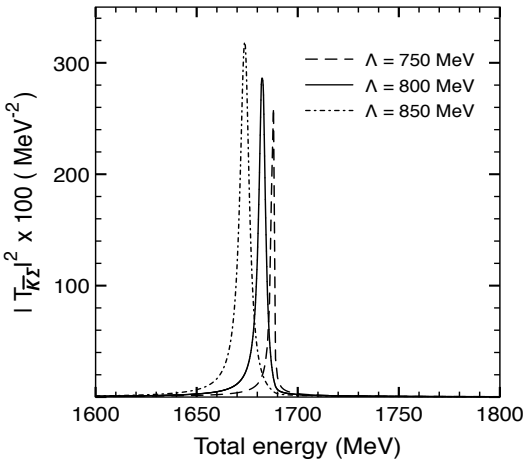

FIG. 7: Variations in the isospin-spin 1/2 squared amplitude of $\bar{K}\Sigma$ channel as a function of the cut-off Λ used in Eq. (19). The peak is associated to $\Xi(1690)$.

from these figures, the results do not vary much, the position and half widths of the resonance changes by $\sim \pm 5$ MeV. The pole positions in the complex plane for both these states are also stable and show a variation of the order of $\sim \pm 5$ MeV.

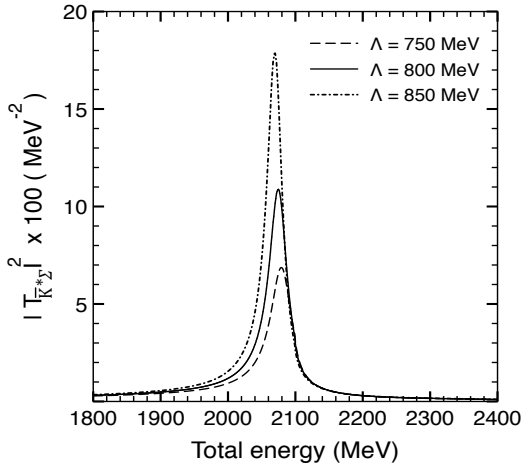

FIG. 8: Same as Fig. 7 but for $\bar{K}^*\Sigma$ in the isospin 1/2, spin 3/2 configuration. The peak seen in this plot is related to $\Xi(2120)$.

The possibility of formation of resonances, like $\Xi(1690)$, due to meson-baryon coupled channel dynamics, can affect relevant cross sections. Such a modification of cross sections, in turn, can be useful in understanding the subthreshold $\Xi(1314)$ production observed in Ar+Kcl collisions at 1.76 A GeV (the threshold in nucleon-nucleon collisions is 3.74 GeV) by the HADES Collaboration [24]. The measured Ξ^- abundance is more than one order of magnitude larger than predicted by the statistical model [25] and by the relativistic transport model [26]. An attempt to explain the observed excess of Ξ^- has been presented in Ref. [27], where, with the help of an SU(3) effective Lagrangian model, the authors computed the cross section for the $YY \to N\Xi$, $\bar{K}Y \to \pi\Xi$ and $\bar{K}N \to K\Xi$ reactions. Including these processes in the RVUU transport model the authors obtained the abundance ratio $R_s = \Xi/(\Lambda + \Sigma^0) = 3.38 \times 10^{-3}$, to be compared with the experimental value of $(5.6 \pm 1.2) \times 10^{-3}$. However, the cross sections used for the process $\bar{K}\Lambda \to \pi\Xi$ in Ref. [27] does not account for the $\Xi(1690)$ resonance formation. The inclusion of such an information drastically enhances the $\bar{K}\Lambda \to \pi\Xi$ cross sections in the lower energy region and changes the line shape of the energy dependence, which should be important. This is shown in Fig. 9, which should be compared with Fig. 2 of Ref. [27]. We also show the cross sections for $\pi\Xi \leftrightarrow \bar{K}\Sigma$ in Fig. 9. Using the cross sections obtained here could increase the abundance ratio R_s obtained in Ref. [27], bringing it closer to the experimental value.

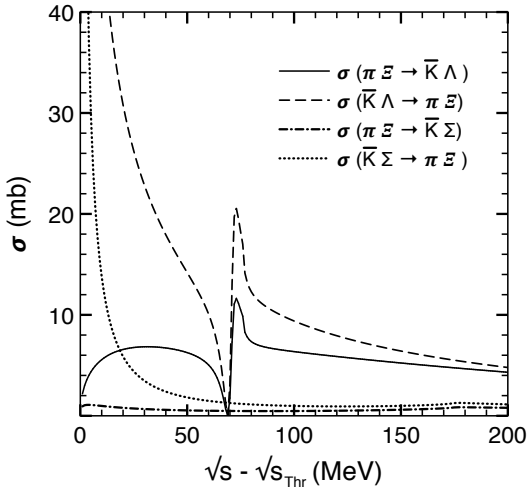

FIG. 9: Cross sections for the $\pi\Xi \leftrightarrow \bar{K}\Lambda$, $\pi\Xi \leftrightarrow \bar{K}\Sigma$ processes. The horizontal axis corresponds to the total energy above the respective threshold of each process. We have used isospin 1/2, spin 1/2 amplitudes to obtain these cross sections.

IV. SUMMARY

We can summarize this manuscript by mentioning that we have shown that pseudoscalar-baryon and vector-baryon coupled channel dynamics generate a resonance which can be well associated to $\Xi(1690)$. The present formalism can explain all the recent experimental findings related to $\Xi(1690)$ with a single parameter of the calculations; a cutoff required to regularize the loop functions. We have also found one broad $1/2^-$ and another narrower $3/2^-$ state in 2050-2100 MeV energy region, and relate the latter one to $\Xi(2120)$. We show that the narrow widths of $\Xi(1690)$ and $\Xi(2120)$ can be understood in terms of their weak couplings to the open channels, which is a result of intricate coupled channel meson-baryon dynamics. It is important to mention here that the vector-baryon dynamics play an essential role in the generation of these poles and in explaining the relevant experimental data. We find that the t-channel interaction and the contact term give dominant contributions to the VB amplitudes. Finally, the existence of such cascades in nature might be an interesting information in statistical models trying to understand the ratio of Ξ^-/Λ production found in heavy ion collisions [24]. We show the cross sections for the processes $\pi\Xi \leftrightarrow \bar{K}\Lambda$, $\pi\Xi \leftrightarrow \bar{K}\Sigma$ which can be useful in studying corresponding in-medium processes.

ACKNOWLEDGEMENTS

K.P.K, A.M.T, F.S.N and M.N gratefully acknowledge the financial support received from FAPESP and CNPq. A.H and H.N thank the support from Grants-in-Aid for

Scientific Research (Grants No. JP26400273(C)) and (Grants No. JP26400275(C), respectively.

Appendix

TABLE IV: $C^{1/2}_{\mathrm{CT,VB}}$ coefficients of the contact term.

	$\rho\Xi$	$\omega\Xi$	$\phi\Xi$	$\bar{K}^*\Sigma$	$\bar{K}^*\Lambda$
$\rho\Xi$	$(F-D)$	0	0	$-\frac{1}{4}(D+F)$	$-\frac{1}{4}(D-3F)$
$\omega\Xi$		0	0	$-\frac{\sqrt{3}}{4}(D+3F)$	$\frac{1}{4\sqrt{3}}(D-3F)$
$\phi\Xi$			0	$-\sqrt{\frac{3}{2}}\frac{(D+F)}{2}$	$-\frac{1}{2\sqrt{6}}(D-3F)$
$\bar{K}^*\Sigma$				$\frac{1}{2}(D+2F)$	$-\frac{D}{2}$
$\bar{K}^*\Lambda$					$-\frac{D}{2}$

TABLE V: $C^{3/2}_{\mathrm{CT,VB}}$ coefficients of the contact term.

	$\rho\Xi$	$\bar{K}^*\Sigma$
$\rho\Xi$	$\frac{(D-F)}{2}$	$-\frac{(D+F)}{2}$
$\bar{K}^*\Sigma$		$\frac{(D-F)}{2}$

TABLE VI: $C^{1/2}_{s,\mathrm{VB}}$ coefficients of the s-channel amplitude, where τ, ν, ξ, ζ are defined in Eq. (A.1).

	$\rho\Xi$	$\omega\Xi$	$\phi\Xi$	$\bar{K}^*\Sigma$	$\bar{K}^*\Lambda$
$\rho\Xi$	$3\tau^2$	$-\sqrt{3}\tau^2$	$\sqrt{3}\tau\nu$	$-3\tau\xi$	$-\tau\zeta$
$\omega\Xi$		τ^2	$-\tau\nu$	$\sqrt{3}\tau\xi$	$\frac{1}{\sqrt{3}}\tau\zeta$
$\phi\Xi$			ν^2	$-\sqrt{3}\nu\xi$	$-\frac{1}{\sqrt{3}}\nu\zeta$
$\bar{K}^*\Sigma$				$3\xi^2$	$\xi\zeta$
$\bar{K}^*\Lambda$					$\frac{1}{3}\zeta^2$

TABLE VII: $C^{1/2}_{u,\mathrm{VB}}$ coefficients of Eq. (10). The definition of different symbols is given in Eq. (A.1).

	$\rho\Xi$	$\omega\Xi$	$\phi\Xi$	$\bar{K}^*\Sigma$	$\bar{K}^*\Lambda$
$\rho\Xi$	$-\alpha^2/2$	$-\sqrt{3}\alpha^2/2$	$-\sqrt{3}\alpha\beta$	$-\gamma+\sqrt{2}\beta\delta$	$\frac{1}{2\sqrt{2}}\zeta\delta\frac{\bar{m}}{M}$
$\omega\Xi$		$\alpha^2/2$	$\alpha\beta$	$-\sqrt{\frac{3}{2}}\beta\delta$	$\frac{1}{\sqrt{3}}\eta\lambda$
$\phi\Xi$			$2\beta^2$	$-\sqrt{\frac{3}{2}}\alpha\delta$	$\frac{2}{3\sqrt{3}}\varepsilon\eta$
$\bar{K}^*\Sigma$				$-\alpha^2/2$	$-\alpha\varepsilon/2$
$\bar{K}^*\Lambda$					$\varepsilon^2/6$

TABLE VIII: $C^{3/2}_{u,\mathrm{VB}}$ coefficients of Eq. (10). The definition of different symbols is given in Eq. (A.1).

	$\rho\Xi$	$\bar{K}^*\Sigma$
$\rho\Xi$	α^2	$\gamma+\beta\delta/\sqrt{2}$
$\bar{K}^*\Sigma$		α^2

TABLE IX: $C^{3/2}_{\mathrm{PBVB}}$ coefficients of the PB $\to$ VB amplitude (Eq. (13)).

	$\rho\Xi$	$\bar{K}^*\Sigma$
$\pi\Xi$	$(F'-D')$	$(D'+F')$
$\bar{K}\Sigma$	$(D'+F')$	$(F'-D')$

$$
\begin{array}{lll}
\alpha=\frac{(F-D)m+2M}{2\sqrt{2}M} & \beta=\frac{Fm+2M}{2M} & \gamma=\frac{Dm[6M-(D-3F)m]}{24M^2} \\
\delta=\frac{(D+F)m+2M}{2\sqrt{2}M} & \varepsilon=\frac{(D+3F)m+6M}{2\sqrt{2}M} & \eta=\frac{6M-(D-3F)m}{8M} \\
\lambda=\frac{(3F-2D)m+6M}{3M} & \tau=\frac{(D-F)m+2M}{4M} & \nu=\frac{Fm-2M}{\sqrt{2}M} \\
\xi=\frac{(D+F)m-2M}{4M} & \zeta=\frac{(D-3F)m+6M}{4M} &
\end{array}
\tag{A.1}
$$

with m and M being an SU(3) average mass for meson and baryon.

TABLE X: $C^{1/2}_{\mathrm{PBVB}}$ coefficients of the PB $\to$ VB amplitude (Eq. (13)).

	$\rho\Xi$	$\omega\Xi$	$\phi\Xi$	$\bar{K}^*\Sigma$	$\bar{K}^*\Lambda$
$\pi\Xi$	$2\,(D'-F')$	0	0	$\frac{1}{2}\,(D'+F')$	$-\frac{1}{2}\,(D'-3F')$
$\eta\Xi$	0	0	0	$-\frac{3}{2}\,(D'+3F')$	$-\frac{1}{2}\,(D'-3F')$
$\bar{K}\Sigma$	$\frac{1}{2}\,(D'+F')$	$\frac{-\sqrt{3}}{2}\,(D'+F')$	$\sqrt{\frac{3}{2}}\,(D'+F')$	$-\,(D'+2F')$	D'
$\bar{K}\Lambda$	$-\frac{1}{2}\,(D'-3F')$	$-\frac{1}{2\sqrt{3}}\,(D'-3F')$	$\frac{1}{\sqrt{6}}\,(D'-3F')$	D'	D'

[1] J. Beringer *et al.* (Particle Data Group), Phys. Rev. D **86**, 010001 (2012).

[2] L. Guo *et al.*, Phys. Rev. C **76**, 025208 (2007); R. Schumacher [CLAS Collaboration], AIP Conf. Proc. **1257**, 100 (2010).

[3] T. Nagae, Nucl. Phys. A **805**, 486 (2008).

[4] M. F. M. Lutz *et al.* [PANDA Collaboration], arXiv:0903.3905 [hep-ex].

[5] K. Abe *et al.* [Belle Collaboration], Phys. Lett. B **524**, 33 (2002).

[6] B. Aubert *et al.* [BaBar Collaboration], Phys. Rev. D **78**, 034008 (2008) [arXiv:0803.1863 [hep-ex]]; B. Aubert *et al.* [BaBar Collaboration], hep-ex/0607043; V. Ziegler, SLAC-R-868.

[7] C. Dionisi *et al.* [Amsterdam-CERN-Nijmegen-Oxford Collaboration], Phys. Lett. B **80**, 145 (1978).

[8] M. Pervin and W. Roberts, Phys. Rev. C **77**, 025202 (2008) [arXiv:0709.4000 [nucl-th]].

[9] L. Y. Xiao and X. H. Zhong, Phys. Rev. D **87**, 094002 (2013) [arXiv:1302.0079 [hep-ph]].

[10] T. Sekihara, PTEP **2015**, 091D01 (2015) [arXiv:1505.02849 [hep-ph]].

[11] N. A. Tornqvist, Phys. Rev. Lett. **67**, 556 (1991).

[12] A. Ramos, E. Oset and C. Bennhold, Phys. Rev. Lett. **89**, 252001 (2002) [nucl-th/0204044].

[13] E. E. Kolomeitsev and M. F. M. Lutz, Phys. Lett. B **585**, 243 (2004) [nucl-th/0305101].

[14] C. Garcia-Recio, M. F. M. Lutz and J. Nieves, Phys. Lett. B **582**, 49 (2004) [nucl-th/0305100].

[15] E. Oset and A. Ramos, Eur. Phys. J. A **44** (2010) 445.

[16] D. Gamermann, C. Garcia-Recio, J. Nieves and L. L. Salcedo, Phys. Rev. D **84**, 056017 (2011) [arXiv:1104.2737 [hep-ph]].

[17] M. Pavon Valderrama, J. J. Xie and J. Nieves, Phys. Rev. D **85**, 017502 (2012) [arXiv:1111.2218 [hep-ph]].

[18] K. Nakayama, Y. Oh and H. Haberzettl, Phys. Rev. C **85**, 042201 (2012) [arXiv:1201.5598 [hep-ph]].

[19] E. J. Garzon and E. Oset, Eur. Phys. J. A **48** (2012) 5.

[20] Y. Oh, Few Body Syst. **54**, 411 (2013) [arXiv:1111.7044 [nucl-th]].

[21] J. B. Gay *et al.* [Amsterdam-CERN-Nijmegen-Oxford Collaboration], Phys. Lett. B **62**, 477 (1976).

[22] A. P. Vorobev *et al.* [French-Soviet and CERN-Soviet Collaborations], Nucl. Phys. B **158**, 253 (1979).

[23] R. J. Hemingway *et al.* [Amsterdam-CERN-Nijmegen-Oxford Collaboration], Phys. Lett. B **68**, 197 (1977).

[24] G. Agakishiev *et al.* [HADES Collaboration], Phys. Rev. Lett. **103**, 132301 (2009); G. Agakishiev *et al.* [HADES Collaboration], Eur. Phys. J. A **52**, no. 6, 178 (2016); G. Agakishiev *et al.* [HADES Collaboration], Eur. Phys. J. A **52**, no. 6, 178 (2016).

[25] E. E. Kolomeitsev, B. Tomasik and D. N. Voskresensky, Phys. Rev. C **86**, 054909 (2012).

[26] L. W. Chen, C. M. Ko and Y. Tzeng, Phys. Lett. B **584**, 269 (2004).

[27] F. Li, L. W. Chen, C. M. Ko and S. H. Lee, Phys. Rev. C **85**, 064902 (2012).

[28] K. P. Khemchandani, H. Kaneko, H. Nagahiro and A. Hosaka, Phys. Rev. D **83** (2011) 114041.

[29] D. Jido, A. Hosaka, J. C. Nacher, E. Oset, A. Ramos, Phys. Rev. **C66**, 025203 (2002).

[30] K. P. Khemchandani, A. Martinez Torres, H. Kaneko, H. Nagahiro and A. Hosaka, Phys. Rev. D **84** (2011) 094018.

[31] P. Maris and P. C. Tandy, Phys. Rev. C **60** (1999) 055214.

[32] P. Maris, Nucl. Phys. A **663** (2000) 621.

[33] K. P. Khemchandani, A. Martinez Torres, H. Nagahiro and A. Hosaka, Phys. Rev. D **85** (2012) 114020.

[34] K. P. Khemchandani, A. Martinez Torres, H. Nagahiro and A. Hosaka, Phys. Rev. D **88** (2013) 114016; K. P. Khemchandani, A. Martinez Torres, H. Nagahiro and A. Hosaka, Int. J. Mod. Phys. Conf. Ser. **26** (2014) 1460060.

[35] G. Ecker, Prog. Part. Nucl. Phys. **35** (1995) 1.

[36] A. Pich, Rep. Prog. Phys. **58** (1995) 563.

[37] E. Oset and A. Ramos, Nucl. Phys. A **635** (1998) 99.

[38] J. A. Oller and E. Oset, Nucl. Phys. A **620** (1997) 438 [Erratum-ibid. A **652** (1999) 407].

[39] T. Hyodo, D. Jido and A. Hosaka, Phys. Rev. C **85**, 015201 (2012).

[40] J. A. Oller and U. G. Meissner, Phys. Lett. B **500**, 263 (2001).

[41] C. Alt *et al.* [NA49 Collaboration], Phys. Rev. Lett. **92**, 042003 (2004)

[42] B. B. Abelev *et al.* [ALICE Collaboration], Eur. Phys. J. C **75**, 1 (2015)